Endothelial Characteristics of Glomerular Capillaries in Normal, Mercuric Chloride-induced, and Gentamicin-induced Acute Renal Failure in the Rat

RUTH ELLEN BULGER, GARABED EKNOYAN, DONALD J. PURCELL II, and DENNIS C. DOBYAN, *Department of Pathology, The University of Texas Medical School and Department of Medicine, Baylor College of Medicine, Houston, Texas 77030*

ABSTRACT A reduction in glomerular capillary endothelial pore size and density has been reported in several models of acute renal failure. It has been suggested that these changes underlie the decrease in glomerular filtration rate and altered glomerular capillary hemodynamics measured in various experimental models of acute renal failure. We have thoroughly quantitated the surface characteristics of glomerular capillaries in control rats and in rats with either mercuric chloride-induced acute renal failure (2 mg/kg body wt) evaluated at 6 and 24 h after administration of the nephrotoxin or with gentamicin (G)[1]-induced acute renal failure evaluated after 8–9 d of 40 mg/kg body wt twice a day. Despite reductions in glomerular filtration rate in the experimental groups, no significant differences were observed between control (C) and any experimental group with respect to percent areas occupied by fenestrated endothelium (C = 53.6±2.7%; 6 h $HgCl_2$ = 50.9±1.9%; 24 h $HgCl_2$ = 53.9±5.7%; G = 56.7±2.4%), by cytoplasmic ridges (C = 31.2±1.5%; 6 h $HgCl_2$ = 29.8±1.9%; 24 h $HgCl_2$ = 30.6±3.1%; G = 26.5±1.5%), nonfenestrated endothelium (C = 15.5±4.0%; 6 h $HgCl_2$ = 19.3±2.0%; 24 h $HgCl_2$ = 15.6±4.3%; G = 16.9±2.3%), in the individual pore area expressed in square nanometers (C = 1,494±75; 6 h $HgCl_2$ = 1,326±48; 24 h $HgCl_2$ = 1,559±130; G = 1,340±101), or in the percentage of total pore area within fenestrated areas that were measured (C = 12.8±0.8%; 6 h $HgCl_2$ = 11.2±0.7%; 24 h $HgCl_2$ = 10.9±0.8%; G = 10.9±0.7%). These results provide quantitative data on the normal glomerular capillary endothelial surface characteristics and suggest that reductions of glomerular filtration rate in acute renal failure are not always associated with alterations in glomerular endothelial capillaries.

INTRODUCTION

Considerable interest has been generated by reports suggesting that alterations in the morphology of the glomerular capillary endothelium play a causative role in the development of acute renal dysfunction in human and experimental models of renal disease. The introduction of a freeze-cracking technique (1) has provided the means for exposing new tissue surfaces, such as the glomerular endothelium, that subsequently can be examined by scanning electron microscopy. This new methodology has allowed for a more thorough evaluation of the glomerular endothelium in a variety of experimental conditions. Using this technique, significant changes in glomerular capillary pore size and pore density have been reported in ischemic (2), glycerol-induced (3), aminoglycoside-induced (4–8), and nephrotoxic (9) models of experimental acute renal failure, as well as in cases of acute renal failure in man (10). Similar changes have been demonstrated in rats with alloxan-induced diabetes (11), in aminonucleoside-induced nephrosis (12), and in rats with spontaneously developing hypertension (13). Previous studies from this laboratory (14) have shown that normal variations in the glomerular endothelium often mimic many of the pathological changes presently being reported in the literature. In this respect, the purpose of the present study was to more thoroughly quantitate the luminal surface characteristics of the glomerular capillary endothelium in normal rats and

Address all correspondence to Dr. R. E. Bulger, Department of Pathology, The University of Texas Medical School at Houston, TX 77025.

Received for publication 1 June 1982 and in revised form 4 March 1983.

in rats subjected to experimental acute renal failure induced by the administration of mercuric chloride or gentamicin.

METHODS

Three groups of Sprague-Dawley male rats weighing between 175 and 275 g were used in this study. All animals had access to food and water until the time of study. The first group of seven rats was used as controls. These animals were injected subcutaneously with an appropriate amount of vehicle alone. Four of the control rats were used for mapping studies while three were used to measure glomerular filtration rate by inulin clearance to document functional normalcy (15). A second group of 16 rats was used in the mercuric chloride-induced acute renal failure study. Mercuric chloride was prepared in a 1 mg/ml solution in normal saline with 0.9% benzyl alcohol and administered subcutaneously in the back of the neck at a dose of 2 mg/kg body wt. Rats were given the appropriate dose of mercuric chloride and killed 6 (n = 5) and 24 h (n = 4) after injection. The glomerular filtration rate was measured from the clearance of inulin in a similarly treated group of seven rats, four studied at 6 and three at 24 h after mercuric chloride administration.

The third group of six rats was used in the gentamicin-induced acute renal failure study. These animals were placed in metabolic cages with free access to food and water. After a 3-d conditioning period, the animals were injected subcutaneously with 40 mg/kg body wt gentamicin twice a day for 8–9 d. 24 h before killing, urine volumes were collected for clearance determination. Blood samples were obtained at the time the animals were killed.

At the time of killing, the animals were anesthetized with an intraperitoneal injection of sodium pentobarbital (40 mg/kg body wt). The kidneys were then fixed by vascular perfusion for 3–5 min using a solution containing 2.5% glutaraldehyde and 2% formaldehyde in 0.04 M sodium cacodylate

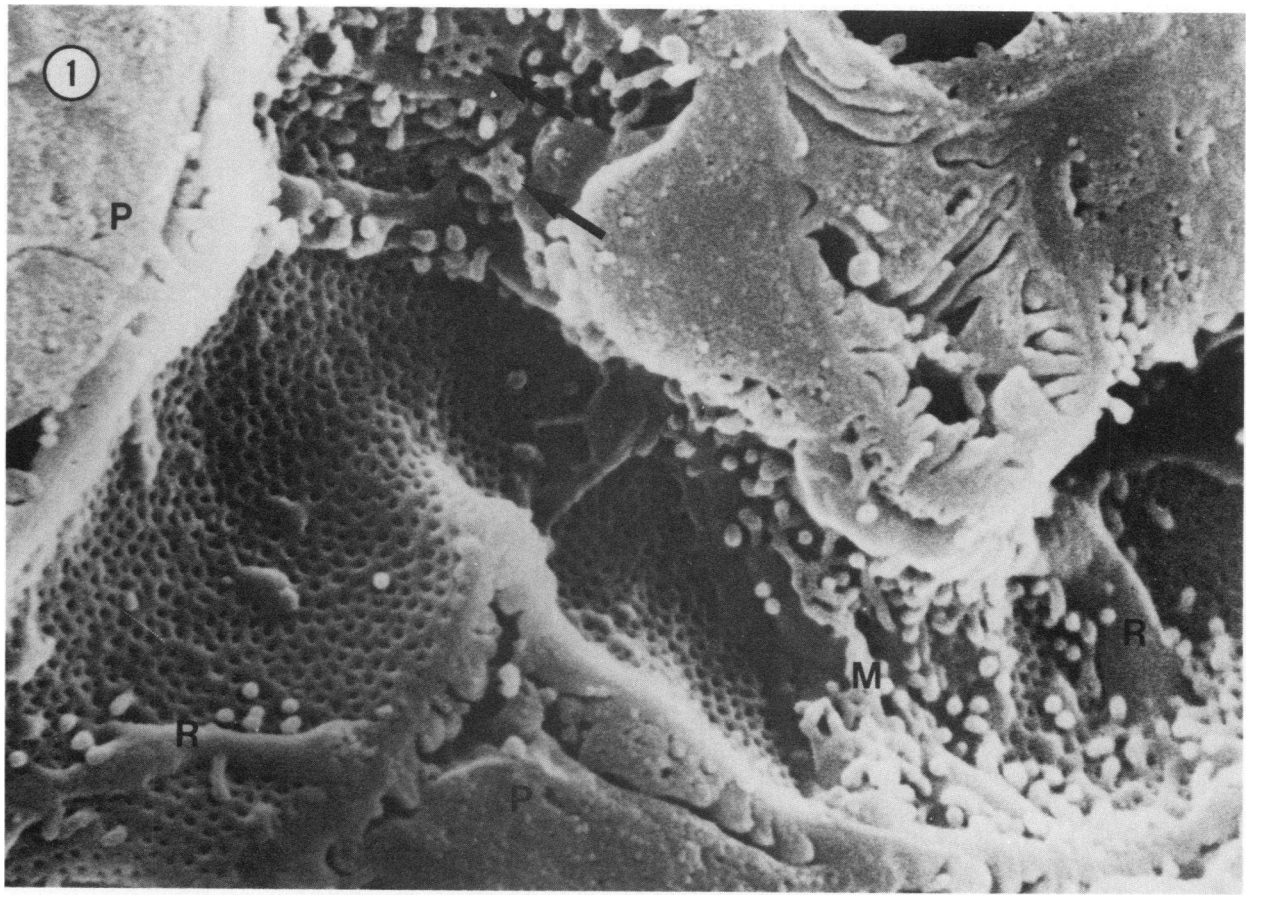

FIGURE 1 Scanning electron micrograph from a control freeze-cracked glomerular capillary showing prominent fenestrated areas. Cytoplasmic ridges (R) encircle the lumen. Microvilli (M) are prominent in certain areas as are pored projections (arrows). Podocytes (P) and their pedicel processes are easily identified. ×21,600.

(pH 7.5), and using a pressure at the perfusion flask of ~180 mmHg. At the pressure used there was no increase in kidney size or vessel size during perfusion (16). Heparinized saline was present only in the final portion of the catheter (PE 100) used for perfusion. Prewashing of the vasculature was not done in order to avoid changes in structure related to this procedure. Following perfusion the kidneys were removed and coded such that all processing of tissue thereafter was done without knowledge of the group of rats from which the tissue samples were obtained. Samples of tissue from each animal were processed for light, transmission, and scanning microscopy as described below.

Light microscopy. After fixation, tissue from each animal was dehydrated, embedded in paraffin, sectioned, and stained routinely with hematoxylin and eosin.

Scanning electron microscopy. Cortical tissue was dissected from each animal and cut into pieces ~1 × 2 × 2 mm. The tissue was postfixed in 1% osmium tetroxide for 90 min, rinsed in three changes of deionized distilled water, and dehydrated in 35 and 50% alcohol solutions for 15 min each and left in 70% alcohol for 3 h. At this point, the samples were freeze-cracked by quickly immersing them individually into liquid nitrogen in a pyrex petri dish insulated in a styrofoam mold. After cracking, the dehydration was completed by placing the tissue pieces in 95% ethanol for 15 min and absolute ethanol for three additional 15-min periods. The tissue was then critical point dried on a Bomar SPC-1500 (The Bomar Co., Tacoma, WA). Using a dissecting stereomicroscope, tissue pieces with shiny surfaces (cracked) were selected and mounted on aluminum stubs with the shiny surface facing up. The stubs were coated with gold palladium for 1.5 min at 40 A using a Denton Vacuum Desk-1 (Denton Vacuum, Inc., Cherry Hill, NJ). Observation of the tissue pieces was made with a JEOL JSM-35 microscope

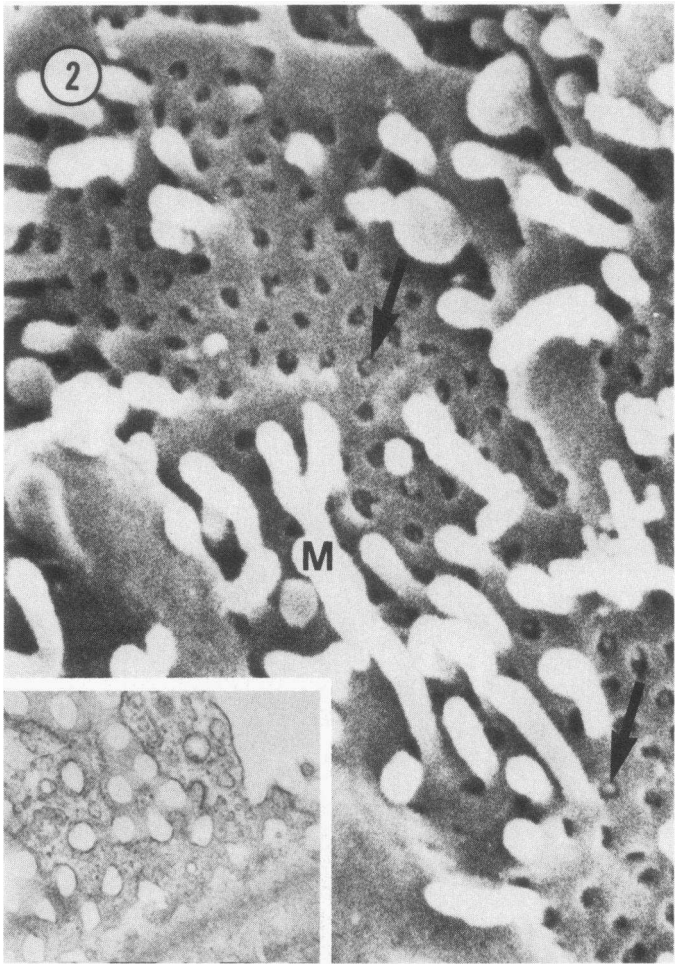

FIGURE 2 Scanning electron micrograph from a control freeze-cracked glomerular capillary. The variation in pore shape can be seen in this picture and by transmission electron microscopy in the inset. Prominent microvilli (M) protrude from the endothelium. In addition, small projections are seen in certain endothelial fenestrae (arrows). ×48,000. *Inset*, ×24,500.

TABLE I

*Endothelial Pore Characteristics of Glomerular Capillaries**

	Pore area	Pore density	Total pore area / Total area measured
	nm^2	$number/\mu m^2$	%
Control	1,494±75	80.7±4.0	12.8±0.8
(n = 4)	(N = 5,680)	(N = 105)	(N = 105)
6 h post-$HgCl_2$	1,326±48	84.9±2.4	11.2±0.7
(n = 5)	(N = 5,562)	(N = 222)	(N = 222)
24 h post-$HgCl_2$	1,559±130	72.8±2.7	10.9±0.8
(n = 4)	(N = 4,207)	(N = 143)	(N = 143)
Gentamicin	1,340±101	87.3±2.6	10.9±0.7
(n = 6)	(N = 4,188)	(N = 199)	(N = 199)

* Expressed as mean of animal values±SEM. N, number of animals studied; n, number of individual measurements obtained in the group of animals studied.
No significant differences were detected between the control group and any of the experimental groups.

(JEOL USA, Analytical Instruments Div., Cranford, NJ) at 25 kV, working distance of 15 mm, and 0° tilt. A mapping study was performed by selecting four cortical and four juxtamedullary glomeruli completely at random from the mounted tissue specimens. The glomeruli to be mapped were first photographed at a low magnification and the positive print was used to select six areas from each glomerulus for more detailed mapping. The areas selected included those regions of the capillary loops that were cracked parallel to the long axis of the capillary and were widely patent. The areas to be studied in more detail were chosen from the print at a magnification too low to see any details of endothelial structure. Pictures of the selected areas were then taken at a fixed magnification of 24,000 times. Of the total prints obtained from each animal, 15 pictures were selected at random for quantitative study.

Two types of quantification were done. First, to determine the surface characteristics of the glomerular capillary endothelium, xerox copies of the 15 randomly chosen micrographs from each animal were made and the following structures were identified and color coded on the xerox copies: cytoplasmic ridges, attenuated areas with endothelial pores, nonfenestrated regions (such as areas over nuclei), and areas not pertaining to this study, such as pedicels or unidentifiable regions. The respective areas were then cut out from these xerox copies and the areas not pertaining to this study were discarded. The pieces from the other three categories were each weighed and used to determine the percent component of each type of structure. These percentages were averaged for each group of animals at the end of the study after the code was broken.

Because of the variation in the shape and size of the endothelial pores, few of which were perfect circles, it was deemed appropriate to quantitate pore size in terms of their surface area rather than surface diameter. To determine endothelial pore area and density, micrographs of the 15 randomly selected examples from each animal were printed at a final magnification of 72,000 times. The prints were then screened by two examiners and the flat areas of the capillary surface parallel to the plane of the photograph showing attenuated endothelium with pores were outlined. Using an electronic digitizer (model 1223, Numonics Corp., Lansdale, PA), the individual pore area of all the pores within the outlined areas of each picture was measured. An average of 1,188 pores per animal was measured. The total area of each of the individual fenestrated areas outlined per print was also measured. To estimate the pore density, the number of pores per unit area was calculated and expressed as number per square micrometers of endothelial surface. In addition, the surface area of all the pores within a delineated area was summed and expressed as a percentage of the total measured area of fenestrated endothelium. After all measurements were obtained, the pictures were decoded and grouped for each animal for subsequent statistical analysis.

Transmission electron microscopy. Superficial, cortical, and juxtamedullary blocks of tissue (1 mm^3) were taken from each animal. The samples were postfixed in osmium tetroxide for 1 h, washed 5 min in 0.1 M sodium cacodylate, dehydrated in a graded series of alcohol solutions, and placed in absolute propylene oxide. The tissues were embedded using Embed-812 and sectioned for transmission electron microscopy with a diamond knife using a Porter Blum microtome. Grid staining was performed using uranyl acetate for 3 min and lead citrate for 5 min as a poststain. Transmission electron micrographs of the glomerular endothelium were taken for correlation with the surface characteristics obtained by scanning electron microscopy.

Statistical methods. All results are expressed as the mean±SEM. Variance analysis was used to determine if significant differences existed between control and the various experimental groups.

RESULTS

Normal structure. A varied spectrum of endothelial surface architecture was observed in the exposed

surface of the normal glomeruli (Fig. 1). Because Fujita et al. (17) have previously described the normal glomerular endothelium using scanning electron microscopy, only a brief description of the normal structural characteristics will be presented. The endothelial surface could be classified according to three main patterns, which together provided a complex structural organization. The first type of endothelial area was characterized by a thin attenuated layer of cytoplasm penetrated by fenestrae (or pores). The fenestrae varied in size, shape, and frequency (Figs. 1, 2, 2 *inset*). Although some of the fenestrae were roughly circular, many were ellipsoidal, angular, or irregular in shape. The fenestrae as seen by scanning electron microscopy frequently contained eccentric projections (Fig. 2) apparently protruding from the base of some pores. No counterpart to these projections could be identified in transmission micrographs (Fig. 2, *inset*). The average area of an endothelial pore was 1,494±75 nm^2. The pore density, (i.e., the number of pores per unit of fenestrated capillary surface area) was 80.7±4/μm^2. The percentage of the capillary surface in these cytoplasmic regions occupied by fenestrae was 12.8±0.8% (Table I).

The second type of area consisted of numerous cytoplasmic ridges or crests oriented predominantly in

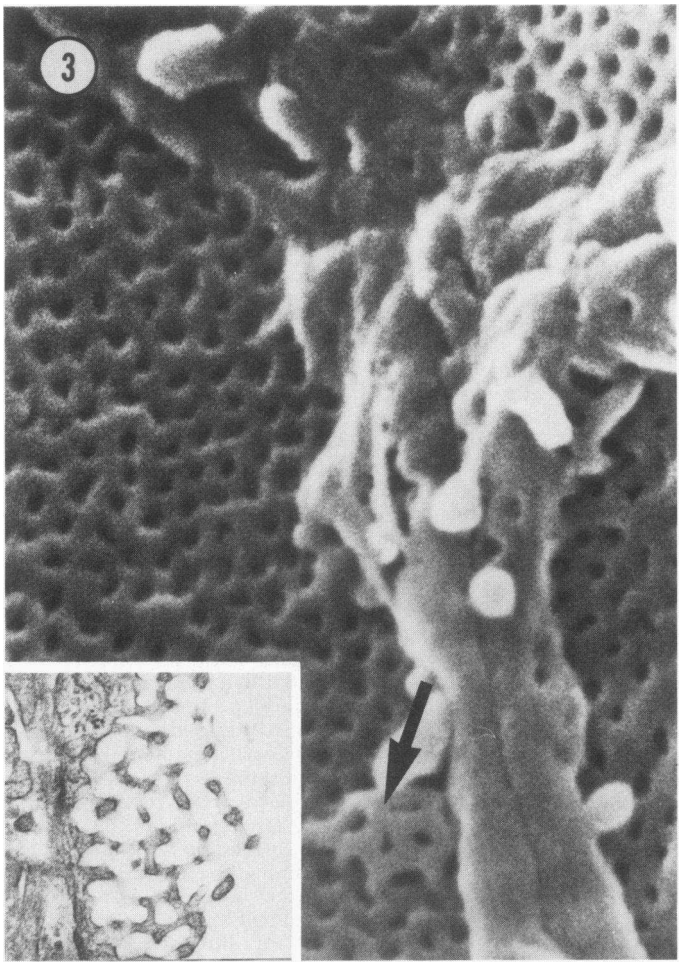

FIGURE 3 Scanning electron micrograph from a control animal showing the lateral borders of three endothelial cells. A prominent cytoplasmic ridge encircles each cell and abuts the ridge from neighboring cells. A pored projection (arrows) is seen adjacent to one peripheral cell ridge. The inset shows a pored projection as it appears in a transmission micrograph. ×60,000. *Inset*, ×25,550.

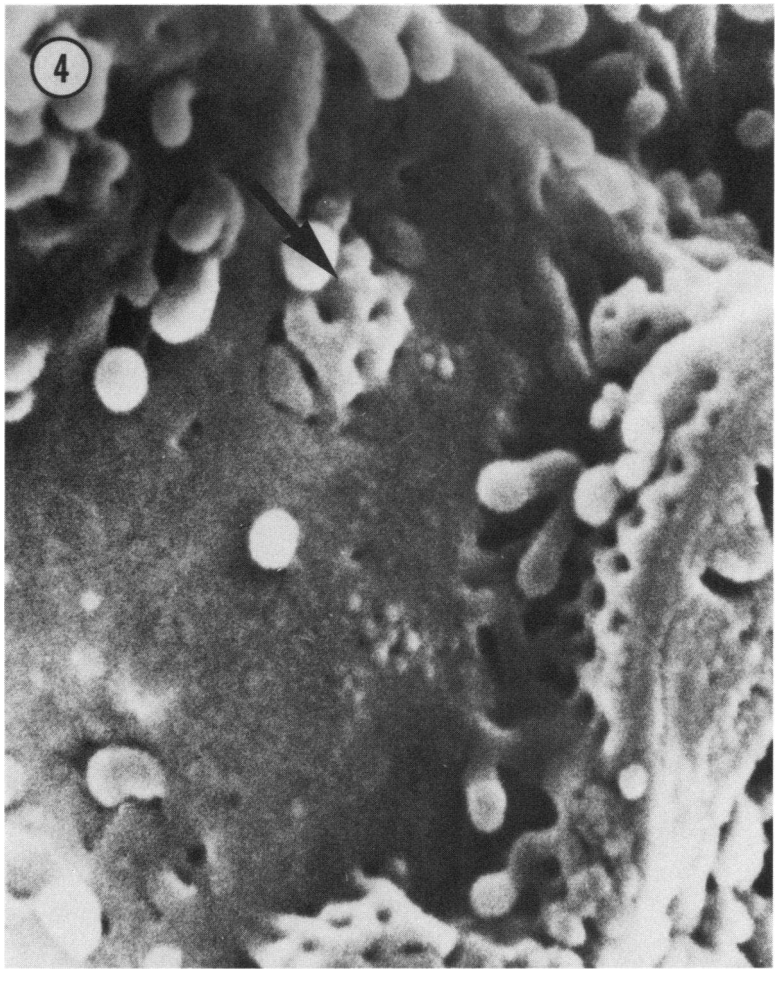

FIGURE 4 Scanning electron micrograph from a control kidney that had been freeze cracked. The majority of the cell surface is nonfenestrated. A pored projection is prominent (arrow). ×60,000.

a circumferential direction (Fig. 1). These primary ridges branched frequently giving rise to less prominent secondary ridges, which connected with neighboring ridges or had extensions that became attenuated and merged into the fenestrated areas of the endothelium. Adjacent ridges abutted at the endothelial cell borders and small overlapping flaps formed at lateral cell contacts (Fig. 3). Some of the primary ridges were studded with microvilli, particularly around their bases (Figs. 2 and 3).

The third type of area consisted of regions essentially devoid of pores (Fig. 4). These areas contained variable numbers of microvilli and what were interpreted as small pits opening on their surfaces. Similar appearing pits were present on the surface of some

TABLE II
*Area of Capillary Surface**

	Fenestrated	Ridges	Nonfenestrated
Control (n = 4)	53.6±2.7	31.2±1.5	15.5±4.0
6 h post-$HgCl_2$ (n = 5)	50.9±1.9	29.8±1.9	19.3±2.0
24 h post-$HgCl_2$ (n = 4)	53.9±5.7	30.6±3.1	15.6±4.3
Gentamicin (n = 6)	56.7±2.4	26.5±1.5	16.9±2.3

* Mean±SEM of capillary surface area of each type expressed as percentage of total area.
No significant differences were detected between the control groups and any of the experimental groups.

cytoplasmic ridges. Transmission electron micrographs showed that these nonfenestrated areas overlaid endothelial cell nuclei, mesangial cells, or areas of normal pedicels.

The percentage of capillary surface area in control animals occupied by thin sheets of fenestrated endothelium was 53.6±2.7%, by cytoplasmic ridges 31.2±1.5%, and by areas without pores 15.5±4.0% (Table II).

An additional specialization of the endothelial cell surface could be found relating to either fenestrated or nonfenestrated regions of the endothelium. These were the so-called pored projections described by Fujita et al. (17) (Fig. 1, 3, 3 *inset*, and 4). These areas were characterized by plates of fenestrae lying above the level of the lining endothelium and in some cases by many microvilli (Figs. 1 and 2). These structures were frequently found in the stalk area near the endothelial cell nucleus as well as throughout the cytoplasm.

In areas where the basal lamina was exposed, due to removal of endothelial cells, a nodular substructure could be identified (Fig. 5) on the endothelial surface of the basal lamina. The nodular substructure was of similar size to the projections seen within some of the endothelial pores.

Glomerular endothelial structure in animals receiving mercuric chloride. Extensive acute tubular

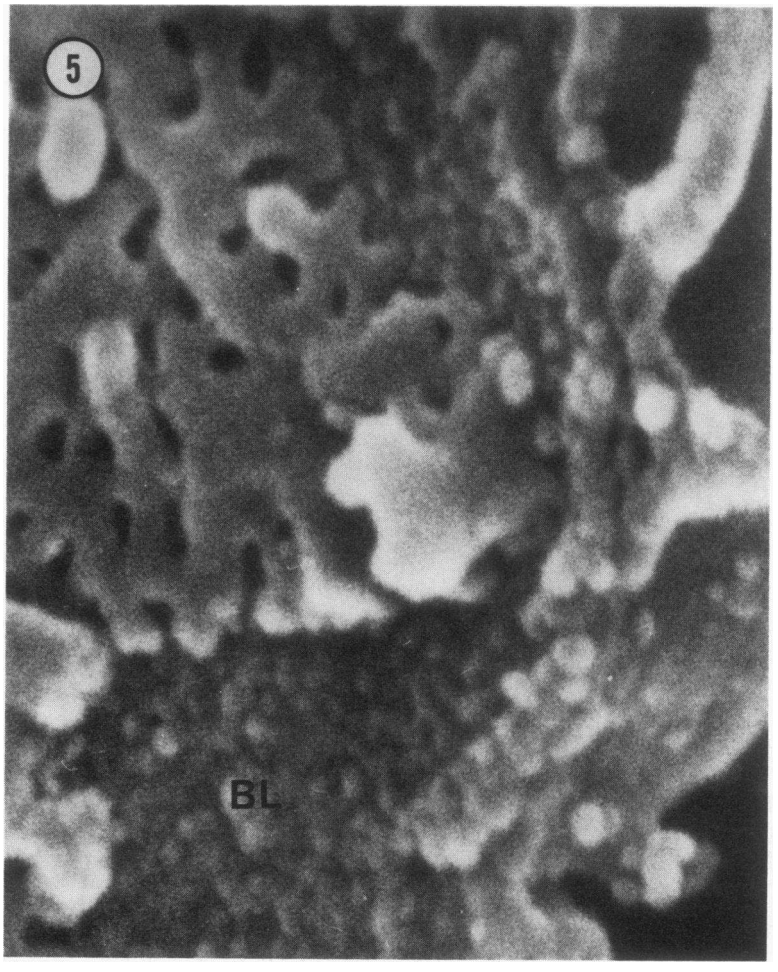

FIGURE 5 Scanning electron micrograph from an area of the capillary in which the endothelium has been removed. The basal lamina (BL) in these exposed areas has a nodular substructure, the nodules being similar in size to the projections previously seen in some endothelial pores. ×96,000.

necrosis was present in the proximal tubule pars recta at 24 h after mercuric chloride administration (Fig. 6). Glomerular filtration rates determined by inulin clearances in microliters per minute per gram kidney weight were 845±30 for controls; 548±64 at 6 h after mercuric chloride; and 134±64 at 24 h after mercuric chloride (18). However, the morphology of the glomerular endothelium seen 6 and 24 h after mercuric chloride administration was indistinguishable from controls (Figs. 7 and 8). The endothelial cell contained the same major types of surface configurations. There were no significant differences between individual pore area, pore density, or percentage of capillary surface area occupied by pore and between control and either experimental time periods studied (Table I). Table II reports the percentage of endothelial surface occupied by fenestrated, ridged, or nonfenestrated endothelium. Again no significant difference could be detected in any of these parameters between control and either experimental group or between the two experimental groups.

Glomerular endothelial structure in animals receiving gentamicin. Extensive injury and necrosis was present in the proximal pars convoluta and a lesser degree of injury was noted in the proximal pars recta (Fig. 9). This extensive necrosis would be consistent with the significant decrease in glomerular filtration rates and the large dose of antibiotic used. Glomerular

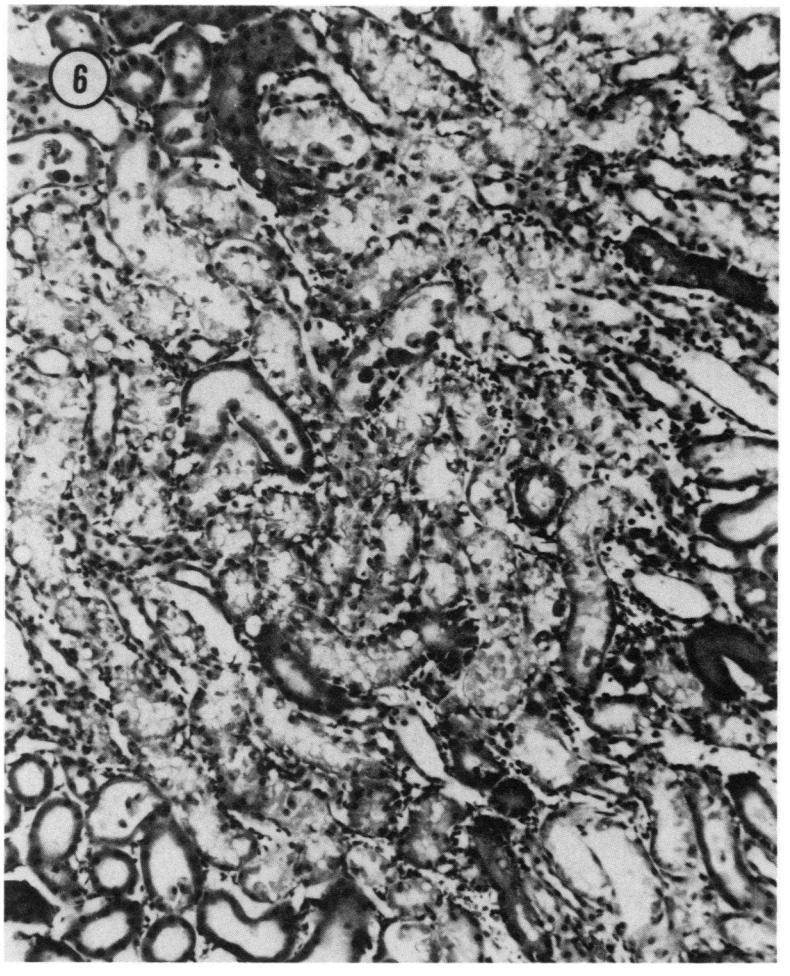

FIGURE 6 Light micrograph taken from an animal given 2 mg/kg body wt of mercuric chloride 24 h before killing. Extensive acute tubular necrosis was seen in the proximal pars recta tubule. Hematoxylin and eosin staining, ×145.

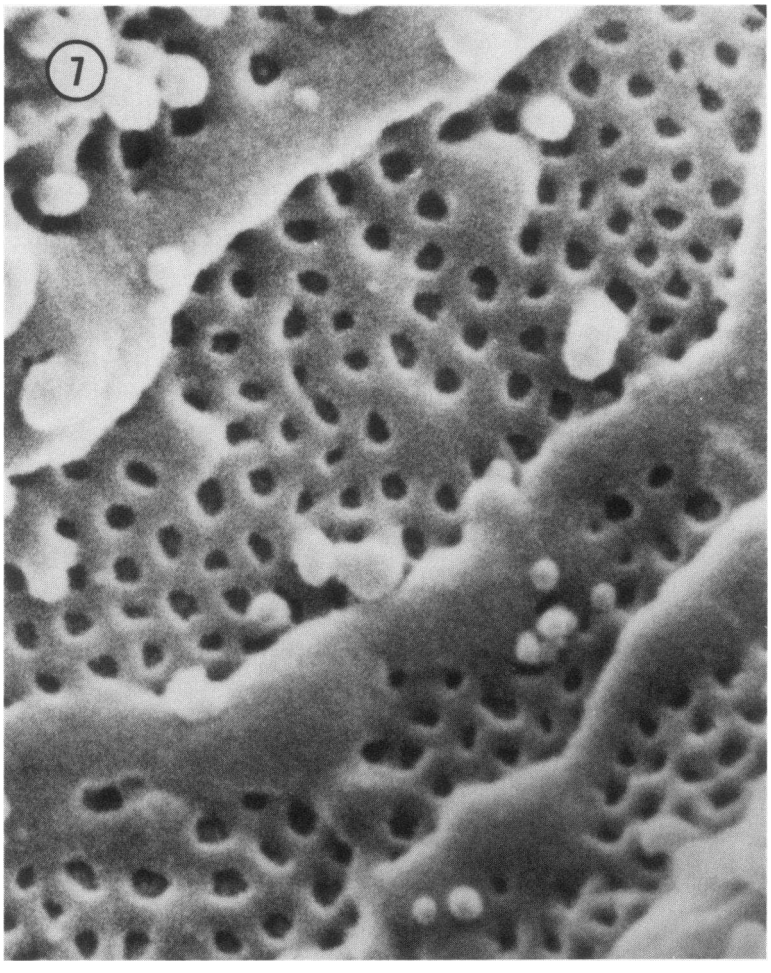

FIGURE 7 Scanning electron micrograph from a fenestrated region of a glomerular capillary 6 h after administration of mercuric chloride. The capillary fenestrae do not differ significantly from those of controls. ×57,600.

filtration rate, determined from the clearance of creatinine, was 102±40 μl/min after 8–9 d of gentamicin administration, a value significantly ($P < 0.001$) lower than that of 1,060±99 μl/min in controls. Despite the extensive tubular alteration and reduction in glomerular filtration rate, the morphology of the glomerular endothelium had no significant differences from control animals with respect to amount of endothelial surface occupied by fenestrated, ridged, or nonfenestrated endothelium (Table II) or by individual pore area, pore density, or percentage of capillary surface area occupied by pores (Table I). However, a larger variation in pore size was seen (Figs. 10, 11, and 12). In certain areas, extremely large pores (maximum area of 3,869 nm^2) were also present (Fig. 12). In addition, the presence of an increased number of pored projections was noted.

DISCUSSION

The three-dimensional architecture of the normal rat glomerular capillary endothelium observed in this study is similar to that described by others (17). No previous study, however, has provided detailed quantitative data of the components of this complex structure. The normal endothelial surface is composed of three main types of surface structures. The predominant component is the attenuated area with fenestrae

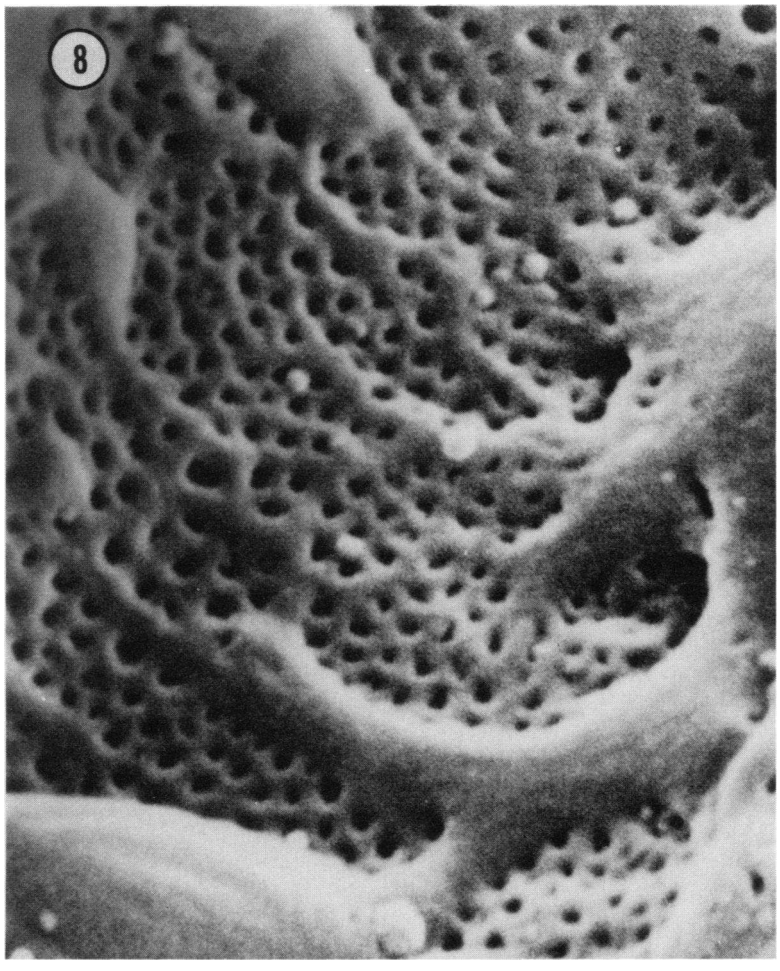

FIGURE 8 Scanning electron micrograph from a fenestrated region of a glomerular capillary 24 h after administration of mercuric chloride. The capillary fenestrae do not differ significantly from those of controls. ×60,000.

that occupies slightly over half the intraluminal surface, with ~12% of this area being occupied by fenestral openings. The fenestrated areas are separated by cytoplasmic ridges that occupy about a third of the endothelial surface area, while the remaining area of ~15% of the capillary surface area is lined by nonfenestrated endothelium, which frequently overlies the cell body and its organelles. This type of quantitation is essential for studies that seek to correlate glomerular function and structure. This is of particular importance, since several recent studies reported decreases in the size and density of endothelial fenestrae in various models of acute renal failure as determined by scanning electron microscopy of freeze-cracked glomeruli. Decreases in glomerular endothelial fenestral size and density have been reported after administration of uranyl nitrate (9), gentamicin (4–8), other aminoglycoside antibiotics (6–8), and glycerol (3) in rats, in human acute renal failure (10), and in ischemic acute renal failure in the dog (2). Decreases in endothelial size and density have been reported in spontaneously hypertensive rats when compared with control (WKY) rats, even before the development of differences in blood pressure (13), as well as in rats made diabetic with alloxan (11). These structural changes, which have been observed in a variety of conditions associated with reduction in glomerular filtration rate, have been construed as evidence for an anatomical basis of altered glomerular capillary dynamics. A decrease in ultrafiltration coefficient has been measured

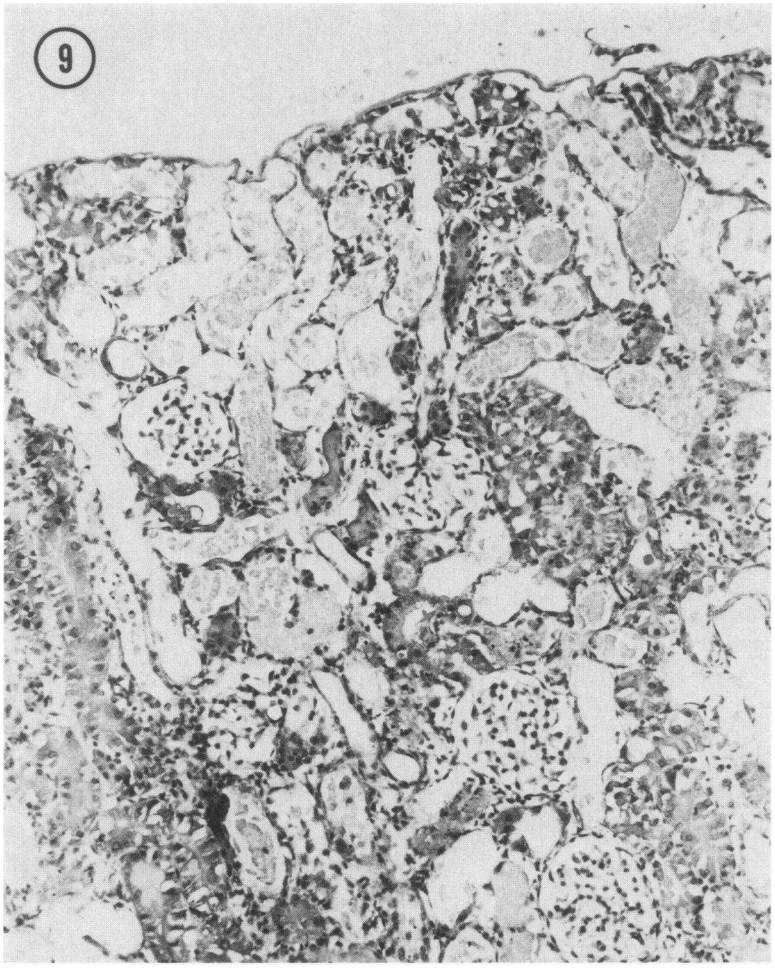

FIGURE 9 Light micrograph from an animal receiving gentamicin showing extensive cell necrosis in the proximal pars convoluta. Hematoxylin and eosin staining, ×150.

in renal failure induced by uranyl nitrate (19), by gentamicin (20), and by ischemia (2). It has been proposed that the reduction in endothelial fenestral size and density underlie the decrease in ultrafiltration coefficient (K_f) measured in these different models of acute renal failure (4–9). The relationship between these ultrastructural lesions and changes in ultrafiltration is unclear, and concern has been expressed that tissue fixation conditions and photographic field selection may influence the assessment of endothelial changes by scanning electron microscopy (21). We have tried to circumvent some of these problems by measuring surface area of the pores rather than diameter of the pores, which is difficult to assess given the irregularity in the shape of pores (Figs. 1, 2, 2 *inset*). Additionally, the large numbers of pores measured in this study (4,188–5,680 pores per group of animals studied, Table I) should have helped eliminate bias in pore selection.

Although most investigators have used higher doses of mercuric chloride, the 2 mg/kg mercuric chloride dose used in this study has been shown to result in acute renal failure in rats (18, 22) and in dogs (23). DiBona et al. (22) measured a decrease in inulin clearance in microliters per minute per 100 g body weight from 987±285 in controls to 585±134 in animals 24 h after administration of 2 mg/kg $HgCl_2$ (blood urea nitrogen went from 18±2 to 32±5). A similar decrease was noted by Eknoyan et al. (18), who observed a drop in inulin clearance from 845±30 μl/min per g kidney wt in control rats to 134±64 24 h after the same dose of mercuric chloride was administered. At that time period 67.1±4.5% of the proximal pars recta cells were

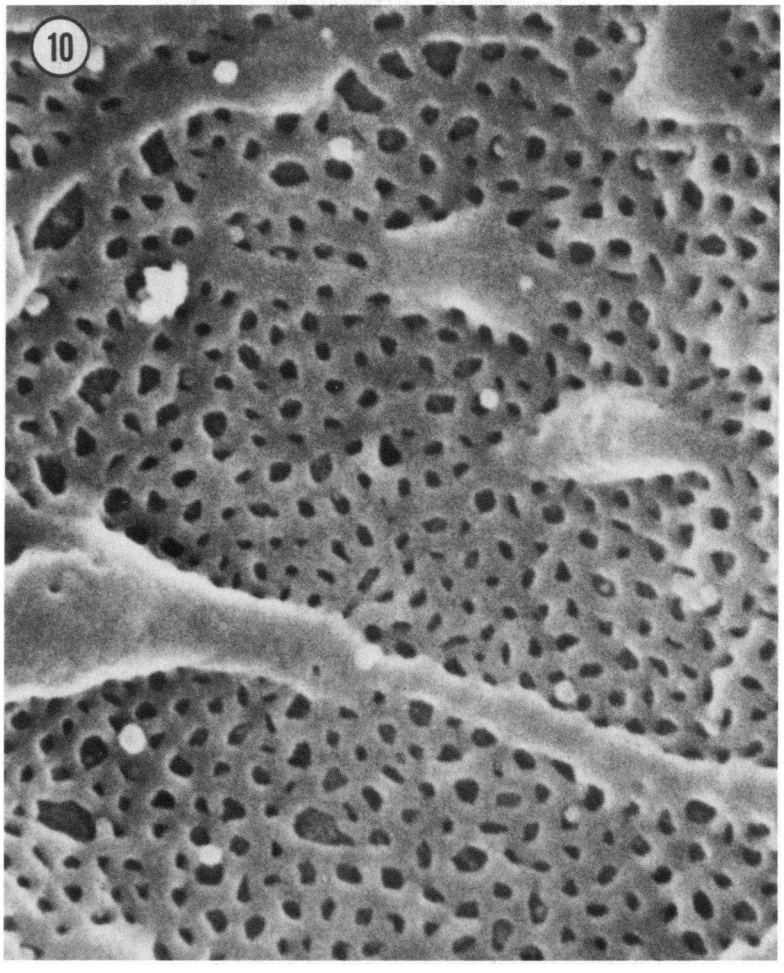

FIGURE 10 Scanning electron micrograph from a fenestrated region of a glomerular capillary from a gentamicin animal showing the variation in pore size seen in these animals. ×40,800.

necrotic (18). This low dose of mercuric chloride produces a reversible model of acute renal failure, although about half of our rats die usually 2 d after drug administration. Similar results were found using mercuric chloride in dogs in which a 1 mg/kg dose did not consistently produce oliguric acute renal failure, whereas a dose of 4 mg/kg caused frequent death of the animals in the first 24 h (23). In this study (23) it was concluded that 2 mg/kg produced a consistent model of oliguric acute renal failure in dogs. The high dose of gentamicin used in this study (40 mg/kg b.i.d. for 8–9 d) was reflected in the severe reduction in creatinine clearance 102±39 μl/min) and elevation of serum creatinine (5.0±0.6 mg/dl). At the time of killing, extensive necrosis was present in the proximal convolutions (79±3%) and in the proximal pars recta (43±10%) (24). Despite the documented severe reduction in glomerular filtration rate and an extensive degree of tubular necrosis in both models of experimental acute renal failure, we were unable to detect any quantifiable differences from normal in endothelial surface characteristics.

The observation of altered endothelial cells in acute renal failure is not supported by all investigators. Although no quantitation was done, Baylis et al. (20) and Schor et al. (25) reported no obvious abnormalities in the glomerular capillary wall after gentamicin administration. Olsen et al. (26) commented that they were unable to demonstrate consistent differences in diameter and/or density of fenestrae after administration of puromycin aminonucleoside to rats. Solez et al. (10) found no significant endothelial cell abnormalities

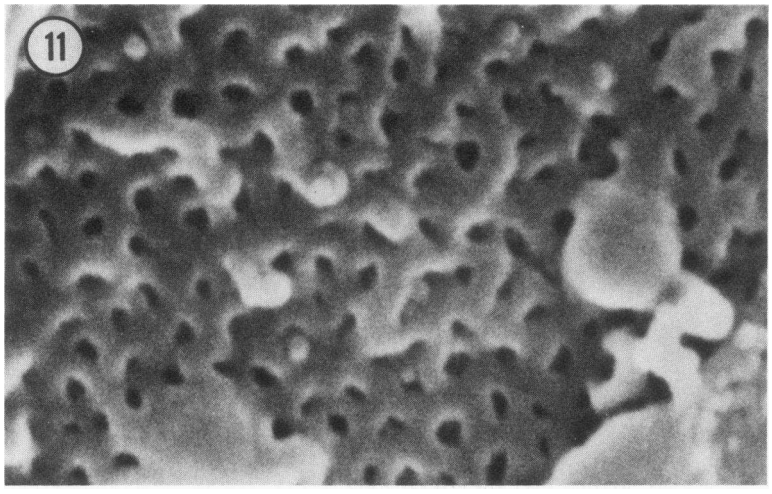

FIGURE 11 Scanning electron micrograph from a fenestrated region of a glomerular capillary from a gentamicin animal showing an area with large pores. ×55,200.

by scanning or transmission electron microscopy in the ischemic model of acute renal failure in rabbits, however, cryofractured specimens were not used in this study.

The studies of Keane and Raij (27) on the role of endothelial fenestrae in glomerular capillary lumen to mesangial traffic of immune complexes are of interest in this regard. They studied the role of mesangial uptake and disappearance of radiolabeled aggregated human IgG in rats with acute renal failure induced by either gentamicin or uranyl nitrate. They found that the capillary mesangial passage of the aggregated IgG was unimpeded in either model in spite of the previously reported major reduction in endothelial fenestral number and surface area in these two situations.

The present study is therefore the first quantitative study of the glomerular endothelium using freeze-cracking techniques that has demonstrated no change in fenestral size or number in two models of acute renal failure. It is possible that mercuric chloride has a different effect on glomerular endothelial cells than that of the other agents previously studied by freeze-cracking (e.g., uranyl nitrate, ischemia), although the

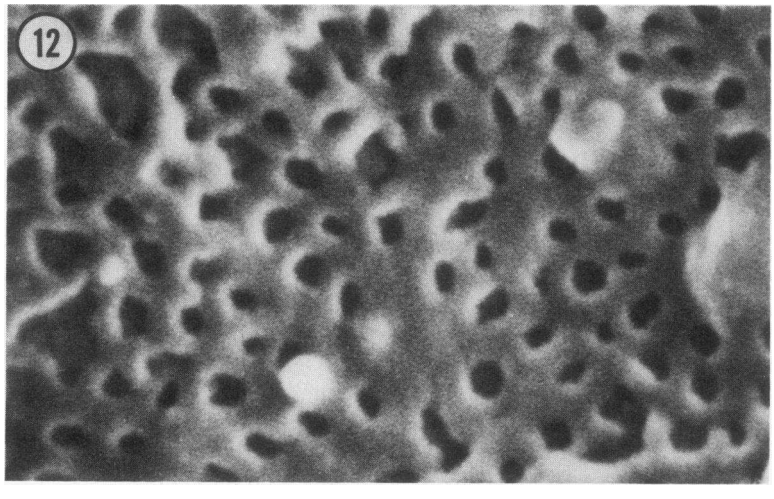

FIGURE 12 Scanning electron micrograph from a fenestrated region of a glomerular capillary from a gentamicin animal with small pores. ×55,200.

glomerular filtration rate drops to the same extent in this model, and oliguria is a component of the renal failure that develops (22). However, we did not identify any significant changes in glomerular capillary structure or in total endothelial pore volume in acute renal failure induced by gentamicin. This differs from the earlier results of others (5–8), who have reported alterations in pore size and density using less rigorous quantitation. Hence, the presumptive role of the glomerular endothelium in the pathogenesis of acute renal failure remains questionable.

ACKNOWLEDGMENTS

The authors wish to thank Dr. Myles L. Mace, Jr. for his advice and help in the use of the digitizer. The authors also wish to thank Ms. Linda Magill, Cherie Gorman, Lee Wallach, and Vicken Sarrafian for their excellent technical assistance.

This work was supported, in part, by National Institutes of Health grant 5R01-AM26134.

REFERENCES

1. Tokunaga, J., M. Edanaga, T. Fujita, and K. Adachi. 1974. Freeze-cracking of scanning electron microscope specimens. A study of the kidney and spleen. *Arch. Histol. Jap.* 37:165–182.
2. Williams, R. H., C. E. Thomas, L. G. Navar, and A. P. Evan. 1981. Hemodynamic and single nephron function during the maintenance phase of ischemic acute renal failure in the dog. *Kidney Int.* 19:503–513.
3. Gattone, V. H., A. P. Evan, and F. C. Luft. 1982. The afferent arteriole in acute renal failure. *Clin. Res.* 30:448*a*. (Abstr.)
4. Avasthi, P. S., J. Huser, and A. P. Evan. 1979. Glomerular endothelial cells in gentamicin-induced acute renal failure (ARF) in rats. *Kidney Int.* 16:771.
5. Avasthi, P. S., A. P. Evan, J. W. Huser, and F. C. Luft. 1981. Effect of gentamicin on glomerular ultrastructure. *J. Lab. Clin. Med.* 98:444–454.
6. Luft, F. C., and A. P. Evan. 1980. Comparative effects of tobramycin and gentamicin on glomerular ultrastructure. *J. Infect. Dis.* 142:910–914.
7. Luft, F. C., and E. P. Evan. 1981. Glomerular filtration barrier in aminoglycoside-induced nephrotoxic acute renal failure. *Renal Physiol.* 3:265–268.
8. Luft, F. C., G. A. Aronoff, A. P. Evan, and B. A. Conners. 1981. The effect of aminoglycosides on glomerular endothelium: a comparative study. *Res. Commun. Chem. Pathol. Pharmacol.* 34:89–95.
9. Avasthi, P. S., A. P. Evan, and D. Hay. 1980. Glomerular endothelial cells in uranyl nitrate-induced acute renal failure in rats. *J. Clin. Invest.* 65:121–127.
10. Solez, K., L. C. Racusen, and A. Whelton. 1981. Glomerular epithelial cell changes in early postischemic acute renal failure in rabbits and man. *Am. J. Pathol.* 103:163–173.
11. Evan, A. P., S. A. Mong, B. A. Connors, and F. C. Luft. 1981. Scanning electron microscopic changes in the filtration barrier of insulin-treated and -untreated alloxan diabetic rats. *Clin. Res.* 29:461*a*. (Abstr.)
12. Avasthi, P. S., and A. P. Evan. 1979. Glomerular permeability in aminonucleoside-induced nephrosis in rats: a proposed role of endothelial cells. *J. Lab. Clin. Med.* 93:266–277.
13. Evan, A. P., F. C. Luft, V. Gattone, B. A. Connors, D. A. McCarron, and L. R. Willis. 1981. The glomerular filtration barrier in the spontaneously hypertensive rat. Hypertension. 3(Suppl. I):I-154–I-161.
14. Purcell, D. J. II, G. Eknoyan, D. C. Dobyan, and R. E. Bulger. 1982. Normal glomerular endothelial morphology. *Kidney Int.* 21:204*a*. (Abstr.)
15. Jamison, R. L. 1968. Micropuncture study of superficial and juxtamedullary nephrons in the rat. *Am. J. Physiol.* 218:46–55.
16. Griffith, L. D., R. E. Bulger, and B. F. Trump. 1967. The ultrastructure of the functioning kidney. *Lab. Invest.* 16:220–246.
17. Fujita, T., J. Tokunaga, and M. Edanaga. 1976. Scanning electron microscopy of the glomerular filtration membrane in the rat kidney. *Cell Tissue Res.* 166:299–314.
18. Eknoyan, G., R. E. Bulger, and D. C. Dobyan. 1982. Mercuric chloride-induced acute renal failure in the rat. I. Correlation of functional and morphological changes and their modification by clonidine. *Lab. Invest.* 46:613–620.
19. Blantz, R. C. 1974. Mechanism of acute renal failure (ARF) after uranyl nitrate (UN). *Clin. Res.* 22:517*a*. (Abstr.)
20. Baylis, C., H. R. Rennke, and B. M. Brenner. 1977. Mechanisms of the defect in glomerular ultrafiltration associated with gentamicin administration. *Kidney Int.* 12:344–353.
21. Whelton, A., and K. Solez. 1982. Aminoglycoside nephrotoxicity—a tale of two transports. *J. Lab. Clin. Med.* 99:148–155.
22. DiBona, G. F., F. D. McDonald, W. Flamenbaum, G. J. Dammin, and D. E. Oken. 1971. Maintenance of renal function in salt-loaded rats despite severe tubular necrosis induced by $HgCl_2$. *Nephron.* 8:205–220.
23. Baehler, R. W., T. A. Kotchen, J. A. Burke, J. H. Galla, and D. Bhathena. 1977. Considerations on the pathophysiology of mercuric chloride-induced acute renal failure. *J. Clin. Lab. Med.* 90:330–340.
24. Eknoyan, G., H. O. Senekjian, R. E. Bulger, and D. C. Dobyan. 1983. Functional and morphological correlates of protection from gentamicin (G) nephrotoxicity by oral clonidine in the rat. *Kidney Int.* 23: 203.
25. Schor, N., I. Ichikawa, H. G. Rennke, J. L. Troy, and B. M. Brenner. 1981. Pathophysiology of altered glomerular function in aminoglycoside-treated rats. *Kidney Int.* 19:288–296.
26. Olson, J. L., H. G. Rennke, and M. A. Venkatachalam. 1981. Alterations in the charge and size selectivity barrier of the glomerular filter in aminonucleoside nephrosis in rats. *Lab. Invest.* 44:271–279.
27. Keane, W. F., and L. Raij. 1981. Determinants of glomerular mesangial localization of immune complexes. Role of endothelial fenestrae. *Lab. Invest.* 45:366–371.